A humid-air-operable, NO_2-responsive polymer transistor series circuit with improved signal-to-drift ratio based on polymer semiconductor oxidation

Huidong Fan[1,2], Hui Li[1], Jinfeng Han[1], Nathaniel McKeever[1], Junsheng Yu[2], Howard E. Katz[1]*

[1]*Department of Materials Science and Engineering, Whiting School of Engineering, Johns Hopkins University, 3400 North Charles Street, Baltimore, Maryland 21218, United States*

[2]*State Key Laboratory of Electronic Thin Films and Integrated Devices, School of Optoelectronic Information, University of Electronic Science and Technology of China (UESTC), Chengdu 610054, P. R. China*

Abstract

A sub-ppm-sensitive nitrogen dioxide (NO_2) sensing circuit with improved humid air stability was realized incorporating UV-ozone treatment on a poly(bisdodecylquaterthiophene) (PQT-12)/polystyrene (PS) blend film. The circuit consisted of a pair of organic field-effect transistors (OFETs) in series, one OFET with and one without this treatment. In contrast to most previous OFET sensors, the readout was obtained from the voltage V_{out} at a point between the OFETs. The circuit showed a low detection limit (200 ppb) towards NO_2, and greatly reduced voltage drift in the humid environment compared to the current drift of the circuit or the individual OFETs because of the balance of conductance drifts on either side of the readout point, which differs from the existing OFET based sensors. By using V_{out} as the detection parameter, the sensitivity of the circuit approaches 25% and 400% for NO_2 concentration of 200 ppb and 20 ppm, respectively. Moreover, the V_{out} is substantial enough to be easily measured by a voltmeter, which could remove the need for complex equipment (semiconductor analyzer system) for the sensing test. We thus demonstrate a simplified approach to stabilized OFET circuits that could be used in printable, flexible or wearable sensors.

Keywords

sensing circuits, organic field-effect transistor (OFET), nitrogen dioxide sensor, humidity-stable sensors, thiophene polymer

For the past few decades, organic field-effect transistors (OFETs) have attracted tremendous attention as they hold advantageous properties for a variety of applications ranging from

flexible electronic papers, flat panel displays, and various physical and chemical sensors.[1-7] Thanks to their biocompatibility, inherent amplification, low power requirement, and low-temperature processing and operating conditions, OFETs have showed qualitative advantages over the inorganic counterparts.[8] During the past few years, there has been a notable acceleration in the development of organic logic circuits, such as inverters,[9] shift registers,[10] comparators,[11] amplifiers and so on.[12-14] Their applications in organic electronics have been recognized as a key enabler for the internet of things (IOTs) as part of the 'Fourth Industrial Revolution'.[15] Moreover, due to their materials characteristics and device structure, OFET-based organic integrated circuits can offer powerful and unique functionalities in chemical-, physical-, and bio-sensors, which provide the foundation of widespread application in both health and environmental monitoring.[16,17]

Great efforts have been made to enhance the performance of OFET based sensors, either based on single OFET devices or logic circuits, especially via material synthesis, device designs, physical measurements and theoretical understanding.[18-23] Li et al. introduced sulfurs into the side chains of poly(bisdodecylquaterthiophene) (PQTS-12), resulting in the increase of traps in the organic film and decrease of the domain size, both of which could contribute to the higher sensitivity to NO_2.[18] Huang et al. used p-type and n-type materials to construct OFET sensor arrays. Owning to the exhibited opposing responses towards a variety of gaseous analytes, the sensor arrays showed different magnitudes and response directions upon exposure to analytes of different basicity, acidity and polarity.[24] Bao et al. designed a microstructured PDMS dielectric in field effect transistors, resulting in highly flexible monolithic transistor devices with excellent pressure sensitivity.[25] Seo et al. systematically investigated the effects of grain boundary density on the gas sensing properties; the increased grain boundary density of organic semiconductor is beneficial for enhancing responses of OFET gas sensor.[26]

With recent widespread increases in economic activity have come corresponding increases in the combustion of fossil fuels that release toxic gases to the atmosphere.[27] Nitrogen dioxide, known as one of the dangerous fossil fuel emissions during combustion, has been shown to have negative effects on health, including edema, nose and throat irritation. Furthermore, NO_2

is an important factor in the formation of acid rain and photochemical smog.[28]

However, despite their advantages in the sensing area, the stability of the OFET based gas sensors still needs further improvement, especially under a humid environment. It was found that water molecules in humid environments can diffuse into the semiconductor layer and/or the interface between the semiconductor and gate dielectric, where they create both donor- and acceptor-like traps, leading to significant degradation of device performance, manifest as decrease of on-current and mobility.[29] For a p-type NO_2 sensor, the presence of NO_2 will lead to the higher on-current and mobility, which conflicts with the humidity influence, leading to unreliable sensing results. Moreover, laboratory demonstrations of OFET-based gas sensors usually need very complex high-tech equipment, disfavoring their widespread application in practical daily application.

Herein, we describe an OFET-based humidity-stabilized logic circuit, a simple strategy to achieve improved NO_2 sensing performance. Besides the normal electrical parameters (source-drain current, mobility, threshold voltage), we also employ V_{out} in a drift-compensated unipolar series circuit to determine the gas sensitivity. By using V_{out} as the detection parameter, the sensitivity of the circuit approaches 25% and 400% for NO_2 concentration of 200 ppb and 20 ppm, respectively. (The United States government exposure limits are approximately 200 ppb and 1 ppm for long and short term exposure, respectively.) As an operational simplification over our recent publication on stabilized sensing circuits,[30] the configuration reported here does not require illumination to achieve stabilization or improved signal-to-drift ratios. We thus demonstrate a more straightforward approach to stabilized OFET circuits that could be further developed for printable, flexible or wearable sensors.

Results and Discussion

Figure 1(a) shows the schematic structure and the diagram of the OFET-based circuit. OFETs consisting of 10 s UV-ozone treated PQT-12/PS blend film are defined as device A, while the untreated OFETs are defined as device B. According to our previous research, UV-ozone treatment is expected to induce functional groups on the surface of polystyrene (PS) film, and the generated functional groups hold the ability to absorb NO_2 analyte, which is essential for achieving ultrasensitive sensors.[31,32] Meanwhile, our experiments also showed that PQT-12 based OFET

devices were not affected by the UV-ozone treatment; both the device performance and the sensing performance remained unchanged. Thus, a PQT-12/PS blend system was chosen to make devices, and the blend film was exposed to the UV-ozone treatment prior to the electrode fabrication.

As shown in **Figure 1(a)**, devices A and B are connected as a logic series circuit and share the same gate electrode. The typical transfer characteristics of the OFET devices and circuits are tested at a driving voltage (V_{DD}) of -40 V and the gate voltage (V_G) of 20 to -40 V. The output characteristics are tested under a V_{DD} of -40 V and a V_G of 0 to -40 V at a step of -10 V.

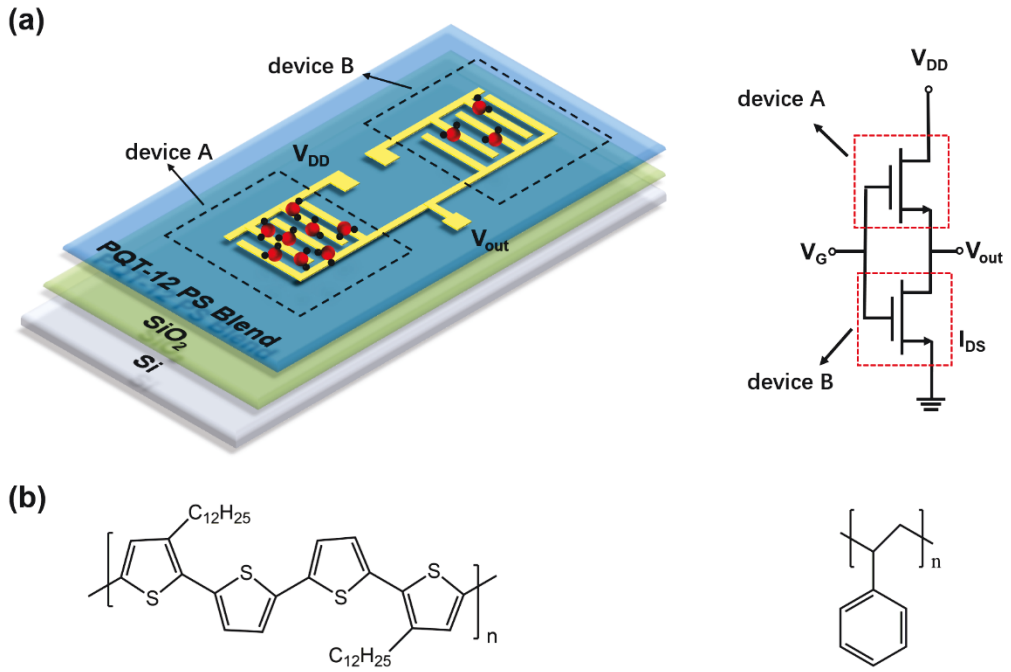

Figure 1. (a) Schematic structure and diagram of the OFET based circuit. (b) The chemical structure of PQT-12 and PS

The effect of UV-ozone on the electrical performance of the individual OFETs is illustrated by the typical output curves shown in **Figure S1** in the Supporting Information. The OFETs show expected p-channel linear and saturation regime characteristics. Moreover, the decreased on-current, mobility and the shift of threshold voltage also indicate that the I-V transfer characteristics are strongly affected by the UV-ozone treatment. Compared to device B, the on-current of device A decreased from 2.1×10^{-6} A to 5.9×10^{-8} A, the threshold voltage shifted from -4 V to -10 V, and the mobility decreased from 9.5×10^{-3} cm^2/Vs to 7.0×10^{-4} cm^2/Vs.

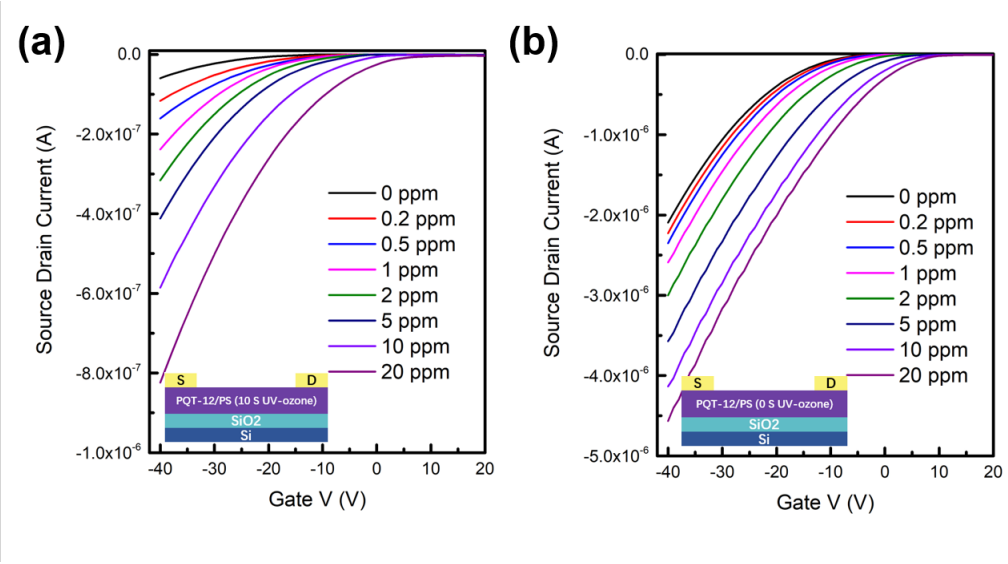

Figure 2. Sensing response of the devices (a)with 10s UV-ozone treatment and (b) without UV-ozone treatment towards different NO_2 concentrations.

These types of individual OFETs were exposed to NO_2 in the test chamber at various concentrations ranging from 200 ppb to 20 ppm. **Figures 2(a)** and **2(b)** show the sensitivity (S) of device A and device B as a function of NO_2 concentration at room temperature; the exposure time of each concentration was 3 min. The sensitivity is calculated by the formula $S = (I_{NO2}-I_{Air})/I_{Air} \times 100\%$, where I_{NO2} is the drain current after exposure to NO_2, and I_{Air} is the drain current before exposure to NO_2. At the concentration of 200 ppb NO_2, the sensitivity of a UV-ozone treated device is 93%, which is nearly 15 times higher than the device without UV-ozone treatment. The mobility increases to 8.3×10^{-4} cm^2/Vs, an increase of 20%. In contrast, without UV-ozone treatment, the sensitivity at 200 ppb is only 6.4%, and the mobility only shows a 2 % increase. At a higher concentration of 20 ppm NO_2, the sensitivity of the UV-ozone treated device is about 1280 %, while the device without UV-ozone treatment is only 118 %, and their mobilities have increases of 360 % and 43 %, respectively. As reported in the literature, after UV-ozone treatment, large densities of oxygen-containing species were introduced onto the surface of the organic semiconducting film, which induced some newly generated functional groups, such as C − O, C=O, and O − C=O.[7,31] These functional groups can efficiently adsorb NO_2 via hydrogen bonding or van der Waals interactions; thus, more charge carries are induced in the channel between source and drain electrode, leading to the drastic increase of the on-current and mobility.[33]

OFETs based on pure PQT-12 films were also fabricated to investigate the influence of UV-ozone treatment on PQT-12. According to the results shown in **Figure S2a**, the electrical performance of the pure PQT-12 devices shows almost no change with or without 10 s UV-ozone treatment. To further illustrate the influence of UV-ozone treatment, each of two devices were exposed to certain concentrations of NO_2 for 3 min. As shown in **Figure S2b**, the two devices show almost the same response to NO_2, which means that 10 s UV-ozone treatment barely affected the PQT-12 materials. Moreover, to illustrate the instinct reason of the different sensing response, the morphology of the PQT-12/PS blend film (with or without 10 s UV-Ozone treatment) was characterized with atomic force microscopy (AFM) (Bruker, Dimension 3100) in tapping mode. As shown in **Figure S3**, PQT-12/PS blend film without 10 s UV-Ozone treatment exhibits a smooth surface with a root mean square (RMS) of 0.593 nm, and the RMS of the film with 10s UV-Ozone treatment is 0.632 nm. There is almost no change of the surface roughness since we only carry out 10 s UV-Ozone treatment. Thus, we can assume that the excellent sensing performance of device A was attributed to the newly generated functional groups in PS.

Since the PS-blended devices with and without UV-ozone treatment showed very different sensitivities towards NO_2, their connection in a logic series circuit leads to the reassignment of the voltage drops across them on exposure to NO_2, shifting V_{out}. Furthermore, for the UV-ozone treated device, the conductance increase resulting from exposure to NO_2 is much larger than the conductance decrease (drift) induced by humidity, even at a lower NO_2 concentration of 200ppb, which can be seen from **Figures 2** and **S4**. The downward drift from humidity is about 35% (RH~75 %), but the upward conductance response in 200 ppb NO_2 is over 80 %. For the untreated device, the downward drift is around 20% in humid environment (RH~75 %), and the conductance increase from 200 ppb NO_2 is a negligible 6.4 %. Thus, the V_{out} response from NO_2 is relatively stabilized even in a humid atmosphere. This is in contrast to a current response to NO_2, which would be diminished by the current degradation caused by humidity. A possible further degradation in response could be caused by the chemical reactivity of the combined adsorbed NO_2 and water.

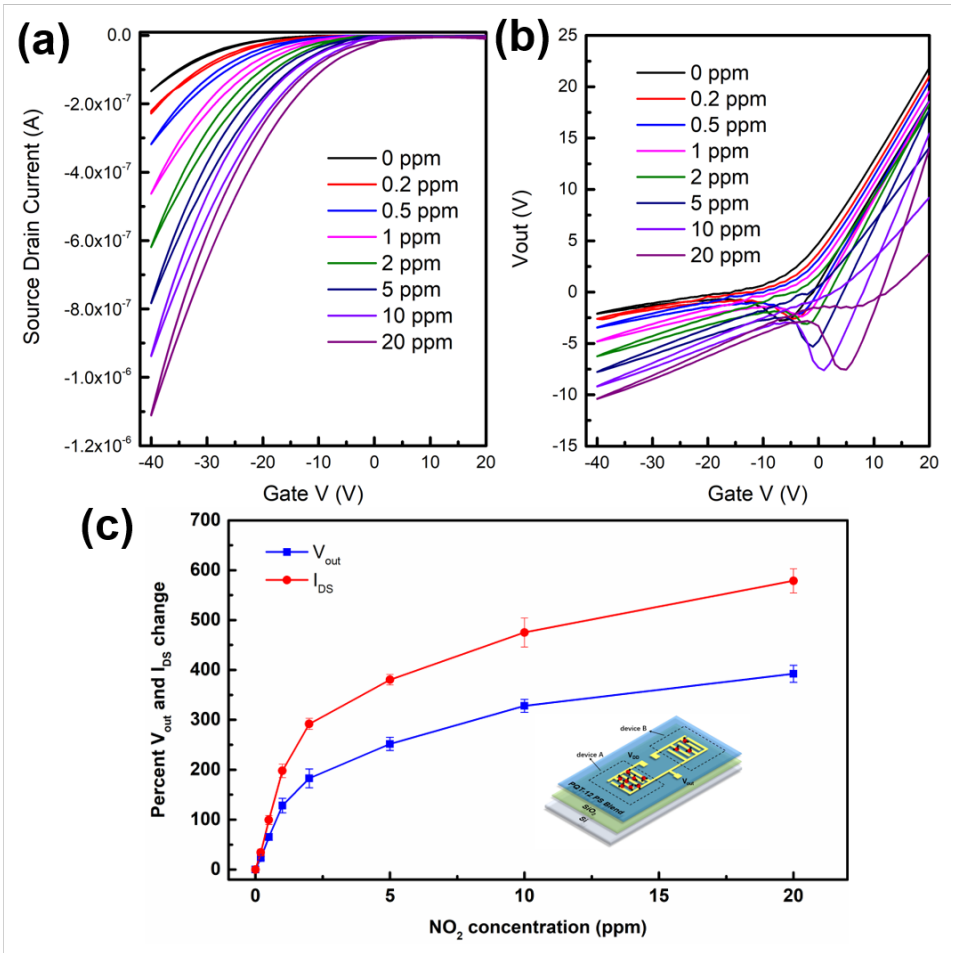

Figure 3. (a)I_{DS} and (b) V_{out} of the logic series circuit when exposed to different NO_2 concentrations; (c)Percent change of V_{out} and I_{DS} when exposed to different NO_2 concentrations.

Table 1. Percent V_{out} and I_{DS} change of the logic series circuit when exposed to NO_2

	0.2 ppm	0.5 ppm	1 ppm	2 ppm	5 ppm	10 ppm	20 ppm
V_{out}	23.1±3.4	65.3±6.7	128±15	183±19	252±13	328±13	392±17
I_{DS}	34.1±6.9	99.5±9.1	198±13	292±11	380.±11	475±29	579±24

As shown in **Figure 1**, the two kinds OFET devices were connected in series circuits. The circuits were tested for 20 cycles to verify the stability of both the on-current and the V_{out} under ambient air, as shown in **Figure S5**, Then the response towards NO_2 at concentrations ranging from 200 ppb to 20 ppm were systematically investigated (3 min for each concentration), as shown in **Figure 3 and Table 1**. The I_{DS} showed a response of 35% under 200 ppb exposure, and 580% under 20 ppm exposure. At 200 ppb, V_{out} increased from 2.09 V to 2.61 V, which is about a 24% increase. With the increase of NO_2 concentration, we see the continuous response

of V_{out}, and at 20 ppm, V_{out} finally reached 10.40 V, that is nearly 400% change. Even though the percent change of V_{out} is not that large, it is still comparable to the change of I_{DS}, with the added advantage that series circuit effectively decreased the influence of background drift, which usually results from the instability of the OFET devices. Finally, by utilizing this kind of logic series circuit, we were easily able to use a common voltmeter to directly read the V_{out} and detect 200 ppb NO_2. Additionally, the hysteresis of the transfer characteristics also shows obvious change during the exposure to NO_2, and it becomes larger along with the increase of NO_2 concentration. One possible mechanism is that the observed hysteresis may due to the desorption of NO_2 molecules during the reverse sweep. Another is that charges induced by NO_2 may also equilibrate to bias voltages and cause bias stress.

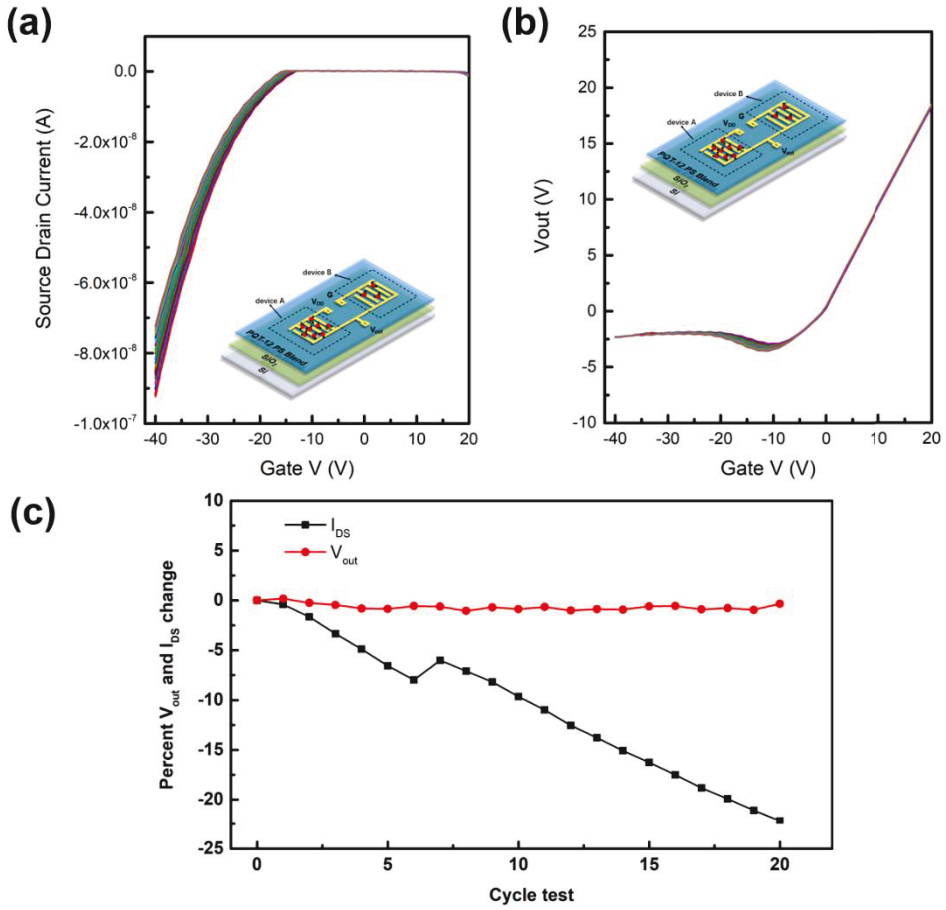

Figure 4. (a)I_{DS} and (b) V_{out} of the logic series circuit when exposed to humid environment for 10 min. (c) Percent change of I_{DS} and V_{out} under humid environment.

Moreover, compared to a single OFET-based gas sensor, our logic circuit showed markedly improved stability while working in a humid environment because of the decreased influence

of the background drift. To demonstrate this, a very wet tissue was put into the test chamber to create a highly humid environment. The single OFET devices were put inside to test their humidity-induced drift by testing their transfer characteristics every 120 s. After 10 min, the relative humidity finally reached 75%. As shown in **Figure S4**, both devices showed decrease of on-current and mobility and shift of the threshold voltage. Water molecules can diffuse into the semiconductor layer and/or the interface between the semiconductor and gate dielectric, where they create both donor- and acceptor-like traps, leading to significant degradation of device performance, manifest as decrease of on-current and mobility.[34] Such devices would not be practical for use as gas sensors to test unknown quantities of analytes in high humidity because of the unreliability of measured parameters, However, after connecting these two devices in a logic series circuit, because the two devices showed similar decreases in electrical conductance, there is no obvious the reassignment of the voltage drop, leading to a stable V_{out} under humid environment. As shown in **Figure 4**, after being tested in the humid environment for 20 cycles (tested every 30 s, RH increased from 15% to 75%), the I_{DS} has a decrease of 21%. In contrast, there is almost no change for the V_{out}, which means that this logic series circuit can suppress the interference of water molecules during the test.

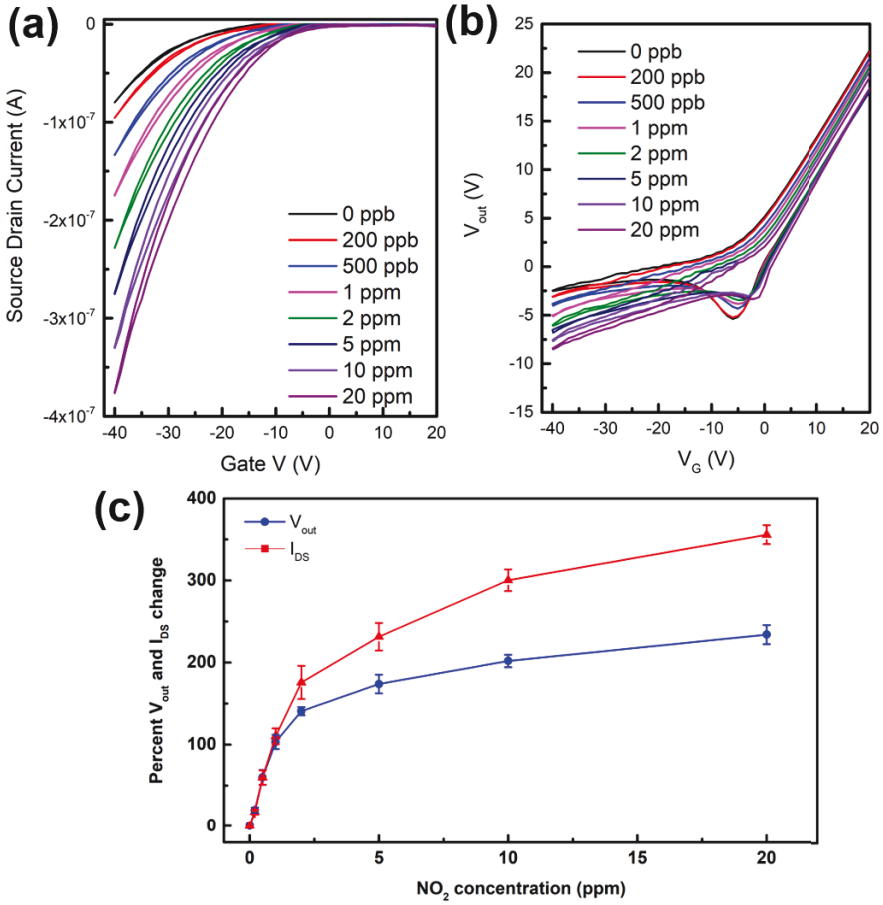

Figure 5. After being exposed to humid environment, (a)I_{DS} and (b) V_{out} of the logic series circuit when exposed to different NO_2 concentrations; percentage change of (c) V_{out} and I_{DS} when exposed to different NO_2 concentrations.

Table 2. After being tested in the humid environment, percent V_{out} and I_{DS} change of the logic series circuit when exposed to NO_2

	0.2 ppm	0.5 ppm	1 ppm	2 ppm	5 ppm	10 ppm	20 ppm
V_{out}	20.1±3.4	59.3±9.1	103±9	140±5	174±11	203±8	235±12
I_{DS}	18.0±3.1	59.9±8.7	110±10	176±20	231±17	300±13	356±11

Furthermore, after being stored in the humid environment for 10 min, the sensitivity of the above circuit towards NO_2 was tested. As mentioned above, the circuit was exposed to various concentrations of NO_2 ranging from 200 ppb to 20 ppm, and the result is shown in **Figure 5** and **Table 2**. We still get the obvious response of I_{DS} and V_{out}, at 200 ppb; the I_{DS} showed a response of 20% under 200 ppb exposure, and 360% under 20 ppm exposure. At 200 ppb, V_{out} increased from 2.5 V to 3.1 V, which is about a 24% increase. With the increase of NO_2 concentration, we see the continuous response of V_{out}, and at 20 ppm, V_{out} finally reached 8.6

V, that is nearly 250%. The percentage change of V_{out} is still comparable to the change of I_{DS}. Moreover, the I_{DS} of the devices showed decrease under humid environment and then increase upon NO_2 exposure, which may lead to the misunderstanding of the gas detection, while for the logic series circuit, the V_{out} remains stable under humid environment and then showed the increase upon NO_2 exposure. The results above demonstrate that by utilizing two devices as a logic series circuit, we can obtain a much more reliable detection result than the common OFET drain current-based sensor.

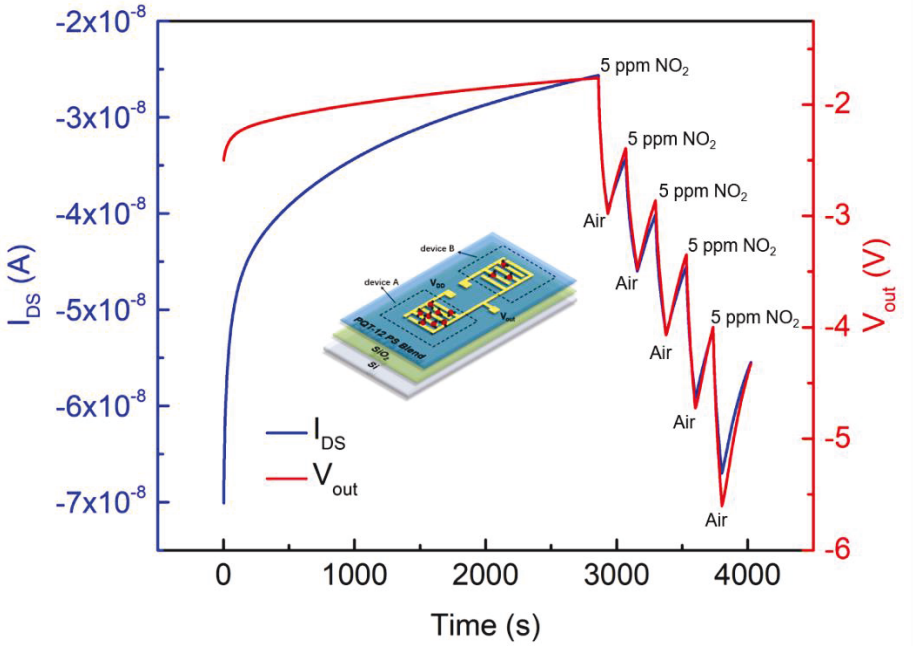

Fig. 6. Real-time I_{DS} and V_{out} responding to different NO_2 concentrations.

Figure 6 shows five cycles of the real-time I_{DS} and V_{out} responding to the dynamic switches of 5 ppm NO_2. The experiments were programmed as follows: 180 s of exposure and subsequent 420 s of dry air purge. Both the V_G and V_{DD} were − 40 V. As shown in **Figure 6**, both the I_{DS} and V_{out} show obvious responses to NO_2 gas exposure; both parameters increase dramatically for every single cycle. For example, during the first cycle, the I_{DS} and V_{out} increase 69% and 54 %, and for the second cycle, I_{DS} and V_{out} showed increase of 61% and 46%, and there is almost no obvious decay for the same concentration exposure, indicating that the circuit shows very good absorption and desorption of NO_2. Although the recovery of the circuit was not complete on the measurement time scale, it could be made so with mild heating or active treatment with a more inert vapor. Meanwhile, the circuit still shows very fast response and holds the ability to detect a low concentration NO_2.

In addition to the response of fresh devices, the environmental stability under ambient atmosphere is another key parameter to the practical application of the sensor devices. As shown in **Figure S6, a**fter being stored in air for 2 weeks, there is a slower drift of the logic series circuits. The I_{DS} of the air stored devices showed a response of 41% under 200 ppb exposure, and 361% under 20 ppm exposure. At 200 ppb, V_{out} increased from 2.57 V to 3.29 V, which is about a 28% increase. With the increase of NO_2 concentration, we see the continuous response of V_{out}, and at 20 ppm, V_{out} finally reached 8.34 V, that is nearly 225% change. The result showed that our device can still work after being stored in ambient atmosphere for 2 weeks.

The sensing selectivity of the logic series circuits towards 5 ppm sulfur dioxide (SO_2), ammonia (NH_3) and hydrogen sulfide (H_2S) were also investigated. As shown in **Figure S7**, the response towards SO_2 is much lower than that of the NO_2, which can be attributed to the lower electron affinity of SO_2. When the logic series circuits were exposed to NH_3 and H_2S, there is a substantial drift toward lower I_{DS} and V_{out} for both two gases. The sensing response towards NO_2, the percent change of V_{out} is not that large, but it is still comparable to the change of I_{DS} when exposed to different gases. Moreover, the logic series circuit effectively decreased the influence of background drift, which usually results from the instability of the OFET devices.

Conclusion

In summary, by combine two different OFETs together, we have successfully fabricated an OFET-based circuit that showed very high sensitivity and very low detection limit (200 ppb) towards NO_2. By utilizing this logic series circuit, we have introduced V_{out} to be considered as another important electrical parameter to determine the gas sensitivity. Moreover, by measuring the V_{out} of the logic series circuit, the gas sensors can be operated with a common voltmeter instead of complex semiconducting equipment. Furthermore, this circuit showed unusual stability towards humid environment (RH~ 75%), and could suppress the interference of water molecules while working as a gas sensor. T represents a significant step toward OFET-based gas sensors precisely detecting NO_2 under such a high humidity. By using V_{out} as the detection parameter, the sensitivity of the circuit approaches 25% and 396% for NO_2 concentration of

200 ppb and 20 ppm, respectively. Thus, we believe that this present strategy can be utilized for the application of low-cost, simple structure, easy operate OFET-based gas sensors with high performance and excellent stability.

Experimental Section

Device Fabrication:

Firstly, heavily doped silicon substrates were kept in piranha solution (a 1:3 mixture of 30 % hydrogen peroxide and sulfuric acid) overnight, followed by ultrasonicating in DI water and isopropanol for 15 min each. After that, the substrates were treated with HMDS. Finally, hexane and isopropanol (ultrasonicating for 15 min each) were used to clean the HMDS-treated substrates. PS (Mw ~ 192,000) was purchased from Sigma-Aldrich and PQT-12 was synthesized by Hui Li. Both the two materials were dissolved in chlorobenzene with a concentration of 8 mg/mL. Before spin-coating the organic semiconductor films, PS and PQT-12 solutions were filtered through PTFE syringe filters (pore size 0.45 μm), then the two solution were mixed together (1:1) and stirred overnight. The mixed solution was spin-coated onto the substrates at a speed of 2000 rpm, after that, the devices were further thermally treated on a hot plate in the glove box at 120 ºC for 20 min to remove solvent residue. Prior to the deposition of electrode, some of the blend semiconductor film were exposed to UV light of 185 and 254 nm (Jelight UVO-Cleaner, model 18) for 10 s. Then 50 nm gold (Au) was thermally deposited as source and drain electrodes on the semiconducting film using shadow masks under 3×10^{-6} Torr at a rate of 0.4 Å/s. Finally, the circuits were completed by connecting the two kind of transistors via Gallium–Indium eutectic (Sigma-Aldrich).

Device Characterization and Sensor Evaluation:

The electrical characteristics of OFET devices with different dielectrics were measured on a custom vacuum probe station using Keithley 4200 source meter (Tektronix) at room temperature (20 ºC). The hole mobility was calculated in the saturation region according to the equation below:

$$I_{DS} = \frac{W}{2L} C_i \mu (V_{GS} - V_{TH})^2 \quad (1)$$

where W (1.1 cm) and L (200 μm) are the channel width and length, and I_{DS} is the drain-source current, respectively. C_i is the capacitance per unit of the dielectric, and V_{GS} is the gate voltage. For the sensing test, the OFET based device was stored in the chamber of the vacuum probe station. Various concentrations of NO_2 were prepared by mixing dry air and 50 ppm standard NO_2, controlled by a mass flow controller. As for the humidity test, a wet tissue was stored in the test chamber to increase the humidity, and the relative humidity was measured by a hygrometer.

Supporting information. The following file is available free of charge. Supporting Information for Fan: Output curves of the PQT-12/PS based OFET devices; output curves of the pure PQT-12 based OFET devices; nitrogen oxide sensing response of the pure PQT-12 based OFET devices; AFM images of the blend film; humidity sensing response of the pure PQT-12 based OFET devices; stability test of the logic circuit under 20 cycles test; stability of the logic circuits in air; selectively of the logic circuits.

Author Information

Corresponding Author

* Howard E. Katz: hekatz@jhu.edu

* Junsheng Yu: jsyu@uestc.edu.cn

Author Contributions

The manuscript was written through contributions of all authors. Fan and McKeever fabricated and tested circuits. Fan was the primary author of the manuscript. Li and Han synthesized materials. Yu and Katz guided the experiments and supervised preparation of the manuscript. All authors have given approval to the final version of the manuscript. The authors declare no competing financial interest.

Acknowledgements

This work was financially supported by the National Key R&D Program of China (Grant No. 2018YFB0407102), the Foundation of National Natural Science Foundation of China (NSFC) (Grant Nos. 61421002, 61675041 & 51703019), and Sichuan Science and Technology Program (Grant Nos. 2019YFH0005, 2019YFG0121, and 2019YJ0178). H. Fan would like to thank the China Scholarship Council (CSC) for financial support (No. 201706070100). H. Li and J. Han (polymer synthesis and device testing methods) and H. Katz (project supervision, data interpretation, and manuscript preparation) were supported by the National Science Foundation, ECCS Division, Award Number 1807293.

References

1. Bonacchini, G. E.; Bossio, C.; Greco, F.; Mattoli, V.; Kim, Y. H.; Lanzani, G.; Caironi, M., Tattoo-Paper Transfer as a Versatile Platform for All-Printed Organic Edible Electronics. *Adv. Mater.* **2018,** *30* (14), 1706091, DOI: 10.1002/adma.201706091

2. Park, J.-S.; Kim, T.-W.; Stryakhilev, D.; Lee, J.-S.; An, S.-G.; Pyo, Y.-S.; Lee, D.-B.; Mo, Y. G.; Jin, D.-U.; Chung, H. K., Flexible full color organic light-emitting diode display on polyimide plastic substrate driven by amorphous indium gallium zinc oxide thin-film transistors. *Appl. Phys. Lett.* **2009,** *95* (1), 013503, DOI: 10.1063/1.3159832

3. Sun, H.; Vagin, M.; Wang, S.; Crispin, X.; Forchheimer, R.; Berggren, M.; Fabiano, S., Complementary Logic Circuits Based on High-Performance n-Type Organic Electrochemical Transistors. *Adv. Mater.* **2018,** *30* (9), 1704916, DOI: 10.1002/adma.201704916

4. Fiore, V.; Battiato, P.; Abdinia, S.; Jacobs, S.; Chartier, I.; Coppard, R.; Klink, G.; Cantatore, E.; Ragonese, E.; Palmisano, G., An integrated 13.56-MHz RFID tag in a printed organic complementary TFT technology on flexible substrate. *IEEE T. CIRCUITS-I.* **2015,** *62* (6), 1668-1677, DOI: 10.1109/TCSI.2015.2415175

5. Shi, W.; Guo, Y.; Liu, Y., When Flexible Organic Field-Effect Transistors Meet Biomimetics: A Prospective View of the Internet of Things. *Adv.Mater.* **2019**, 1901493, DOI: 10.1002/adma.201901493

6. Li, H.; Shi, W.; Song, J.; Jang, H.-J.; Dailey, J.; Yu, J.; Katz, H. E., Chemical and biomolecule sensing with organic field-effect transistors. *Chem. Rev.* **2018,** *119* (1), 3-35, DOI: 10.1021/acs.chemrev.8b00016

7. Huang, W.; Yu, X.; Fan, H.; Yu, J., High performance unipolar inverters by utilizing organic field-effect transistors with ultraviolet/ozone treated polystyrene dielectric. *Appl. Phys. Lett.* **2014,** *105* (9), 139_1, DOI: 10.1063/1.4895121

8. Tang, W.; Huang, Y.; Han, L.; Liu, R.; Su, Y.; Guo, X.; Yan, F., Recent progress in printable organic field effect transistors. *Journal Mater. Chem. C* **2019,** *7* (4), 790-808, DOI: 10.1039/C8TC05485A

9. Kwon, J.; Matsui, H.; Kim, W.; Tokito, S.; Jung, S., Static and Dynamic Response Comparison of Printed, Single-and Dual-Gate 3-D Complementary Organic TFT Inverters. *IEEE Electr. Device L.*

2019, *40* (8), 1277-1280, DOI: 10.1109/LED.2019.2922296
10. Torricelli, F.; Ghittorelli, M.; Smits, E. C.; Roelofs, C. W.; Janssen, R. A.; Gelinck, G. H.; Kovács-Vajna, Z. M.; Cantatore, E., Ambipolar Organic Tri-Gate Transistor for Low-Power Complementary Electronics. *Adv. Mater.* **2016,** *28* (2), 284-290, DOI: doi.org/10.1002/adma.201503414
11. Xiong, W.; Zschieschang, U.; Klauk, H.; Murmann, B. In A 3V 6b successive-approximation ADC using complementary organic thin-film transistors on glass, 2010 IEEE International Solid-State Circuits Conference-(ISSCC), IEEE: 2010; pp 134-135, DOI: 10.1109/ISSCC.2010.5434017
12. Reuveny, A.; Lee, S.; Yokota, T.; Fuketa, H.; Siket, C. M.; Lee, S.; Sekitani, T.; Sakurai, T.; Bauer, S.; Someya, T., High-frequency, conformable organic amplifiers. *Adv. Mater.* **2016,** *28* (17), 3298-3304, DOI: 10.1002/adma.201505381
13. Klauk, H.; Zschieschang, U.; Pflaum, J.; Halik, M., Ultralow-power organic complementary circuits. *Nature* **2007,** *445* (7129), 745, DOI: 10.1038/nature05533
14. Yoo, B.; Jones, B. A.; Basu, D.; Fine, D.; Jung, T.; Mohapatra, S.; Facchetti, A.; Dimmler, K.; Wasielewski, M. R.; Marks, T. J., High-Performance Solution-Deposited n-Channel Organic Transistors and their Complementary Circuits. *Adv. Mater.* **2007,** *19* (22), 4028-4032, DOI: 10.1002/adma.200700064
15. Chang, J. S.; Facchetti, A. F.; Reuss, R., A circuits and systems perspective of organic/printed electronics: Review, challenges, and contemporary and emerging design approaches. *IEEE J. Em. Sel. Top. C.* **2017,** *7* (1), 7-26, DOI: 10.1109/JETCAS.2017.2673863
16. Ren, X.; Pei, K.; Peng, B.; Zhang, Z.; Wang, Z.; Wang, X.; Chan, P. K., A low-operating-power and flexible active-matrix organic-transistor temperature-sensor array. *Adv. Mater.* **2016,** *28* (24), 4832-4838, DOI: doi.org/10.1002/adma.201600040
17. Takeda, Y.; Hayasaka, K.; Shiwaku, R.; Yokosawa, K.; Shiba, T.; Mamada, M.; Kumaki, D.; Fukuda, K.; Tokito, S., Fabrication of ultra-thin printed organic TFT CMOS logic circuits optimized for low-voltage wearable sensor applications. *Sci. Rep.* **2016,** *6*, 25714, DOI: 10.1038/srep25714 (2016)
18. Li, H.; Dailey, J.; Kale, T.; Besar, K.; Koehler, K.; Katz, H. E., Sensitive and Selective NO2 Sensing Based on Alkyl-and Alkylthio-Thiophene Polymer Conductance and Conductance Ratio Changes from Differential Chemical Doping. *ACS Appl. Mater. Inter.* **2017,** *9* (24), 20501-20507, DOI: 10.1021/acsami.7b02721
19. Yamamura, A.; Matsui, H.; Uno, M.; Isahaya, N.; Tanaka, Y.; Kudo, M.; Ito, M.; Mitsui, C.; Okamoto, T.; Takeya, J., Painting Integrated Complementary Logic Circuits for Single-Crystal Organic Transistors: A Demonstration of a Digital Wireless Communication Sensing Tag. *Adv. Electron. Mater.* **2017,** *3* (7), 1600456, DOI: 10.1002/aelm.201600456
20. Zang, Y.; Huang, D.; Di, C. a.; Zhu, D., Device engineered organic transistors for flexible sensing applications. *Adv. Mater.* **2016,** *28* (22), 4549-4555, DOI: 10.1002/adma.201505034
21. Trung, T. Q.; Lee, N. E., Flexible and stretchable physical sensor integrated platforms for wearable human-activity monitoringand personal healthcare. *Adv. Mater.* **2016,** *28* (22), 4338-4372, DOI: 10.1002/adma.201504244
22. Zhou, X.; Niu, K.; Wang, Z.; Huang, L.; Chi, L., An ammonia detecting mechanism for organic transistors as revealed by their recovery processes. *Nanoscale* **2018,** *10* (18), 8832-8839, DOI: 10.1039/c8nr01275j
23. Jang, H.-J.; Wagner, J.; Li, H.; Zhang, Q.; Mukhopadhyaya, T.; Katz, H. E., Analytical Platform To Characterize Dopant Solution Concentrations, Charge Carrier Densities in Films and Interfaces, and Physical Diffusion in Polymers Utilizing Remote Field-Effect Transistors. *J. Am. Soc.* **2019,** *141*

(12), 4861-4869, DOI: 10.1021/jacs.8b13026
24. Huang, W.; Sinha, J.; Yeh, M. L.; Hardigree, J. F. M.; LeCover, R.; Besar, K.; Rule, A. M.; Breysse, P. N.; Katz, H. E., Diverse Organic Field - Effect Transistor Sensor Responses from Two Functionalized Naphthalenetetracarboxylic Diimides and Copper Phthalocyanine Semiconductors Distinguishable Over a Wide Analyte Range. *Adv. Funct. Mater.* **2013,** *23* (33), 4094-4104, DOI: 10.1002/adfm.201300245
25. Schwartz, G.; Tee, B. C. K.; Mei, J.; Appleton, A. L.; Kim, D. H.; Wang, H.; Bao, Z., Flexible polymer transistors with high pressure sensitivity for application in electronic skin and health monitoring. *Nat. Commun.* **2013,** *4* (5), 1859, DOI: 10.1038/ncomms2832 (2013)
26. Seo, Y.; Lee, J. H.; Anthony, J. E.; Nguyen, K. V.; Kim, Y. H.; Jang, H. W.; Ko, S.; Cho, Y.; Lee, W. H., Effects of Grain Boundary Density on the Gas Sensing Properties of Triethylsilylethynyl - Anthradithiophene Field - Effect Transistors. *Adv. Mater. Interfaces* **2018,** *5* (3), 1701399, DOI: 10.1002/admi.201701399
27. Nejat, P.; Jomehzadeh, F.; Taheri, M. M.; Gohari, M.; Majid, M. Z. A., A global review of energy consumption, CO2 emissions and policy in the residential sector (with an overview of the top ten CO2 emitting countries). *Renew. Sust. Energ. Rev.* **2015,** *43*, 843-862, DOI: 10.1016/j.rser.2014.11.066
28. Soni, V.; Singh, P.; Shree, V.; Goel, V., Effects of VOCs on human health. *Air pollution and control*, Springer: 2018; pp 119-142, DOI: 10.1007/978-981-10-7185-0_8
29. Kim, S. H.; Yang, H.; Yang, S. Y.; Hong, K.; Choi, D.; Yang, C.; Chung, D. S.; Park, C. E., Effect of water in ambient air on hysteresis in pentacene field-effect transistors containing gate dielectrics coated with polymers with different functional groups. *Org. Electron.* **2008,** *9* (5), 673-677, DOI: 10.1016/j.orgel.2008.05.004
30. Chu, Y.; Li, H.; Huang, J.; Katz, H. E., High Signal - to - Noise Chemical Sensors Based on Compensated Organic Transistor Circuits. *Adv. Mater. Technol.* **2019**, 1900410, DOI: 10.1002/admt.201900410
31. Huang, W.; Zhuang, X.; Melkonyan, F. S.; Wang, B.; Zeng, L.; Wang, G.; Han, S.; Bedzyk, M. J.; Yu, J.; Marks, T. J., UV–Ozone interfacial modification in organic transistors for high-sensitivity NO2 detection. *Adv. Mater.* **2017,** *29* (31), 1701706, DOI: 10.1002/adma.201701706
32. Someya, T.; Dodabalapur, A.; Huang, J.; See, K. C.; Katz, H. E., Chemical and physical sensing by organic field-effect transistors and related devices. *Adv. Mater.* **2010,** *22* (34), 3799-3811, DOI: 10.1002/adma.200902760
33. Zhang, C.; Chen, P.; Hu, W., Organic field-effect transistor-based gas sensors. *Chem. Soc. Rev.* **2015,** *44* (8), 2087-2107, DOI: 10.1039/C4CS00326H
34. Chabinyc, M. L.; Endicott, F.; Vogt, B. D.; DeLongchamp, D. M.; Lin, E. K.; Wu, Y.; Liu, P.; Ong, B. S., Effects of humidity on unencapsulated poly (thiophene) thin-film transistors. *Appl. Phys. Lett.* **2006,** *88* (11), 113514, DOI: 10.1063/1.2181206

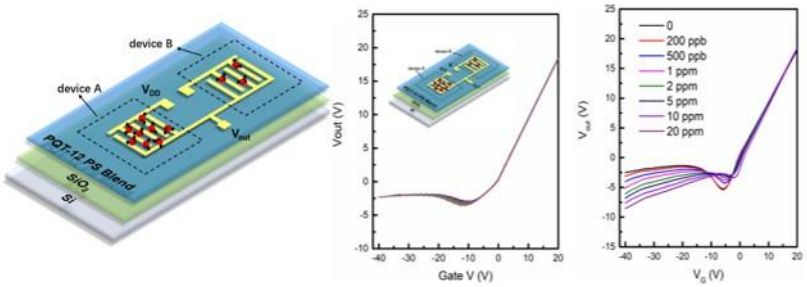
device B
device A
V_{DD}
V_{out}
PQT-12 PS Blend
SiO_2
Si
Vout (V)
Gate V (V)
V_{out} (V)
V_G (V)
0
200 ppb
500 ppb
1 ppm
2 ppm
5 ppm
10 ppm
20 ppm

For TOC Only